Research Square

Preprints are preliminary reports that have not undergone peer review.
They should not be considered conclusive, used to inform clinical practice,
or referenced by the media as validated information.

Preclinical Models for Evaluation of Drug Efficacy against Mycobacterium abscessus

Gaëlle Guiewi Makafe
Trudeau Institute
Tim Low-Beer
Trudeau Institute
Debra Duso
Trudeau Institute
Brian Weinrick
bweinrick@trudeauinstitute.org
Trudeau Institute

Research Article

Keywords: Mycobacterium abscessus, mouse infection, drug efficacy, Nos2, βENaC, parkin, C3HeB/FeJ, morphotype, macrophage

Posted Date: November 23rd, 2026

DOI: https://doi.org/10.21203/rs.3.rs-11706724/v1

License: This work is licensed under a Creative Commons Attribution 4.0 International License.
Read Full License

Additional Declarations: No competing interests reported.

Abstract

Background

Mycobacterium abscessus, a growing cause of non-tuberculous mycobacterial infections, is challenging to treat due to intrinsic drug resistance. More effective therapies are urgently needed. To advance treatments to clinical trials, predictive preclinical models are required but have been difficult to establish in immunocompetent mice. A recent report that individuals with decreased expression of parkin, involved in autophagy regulation, are overrepresented among patients with pulmonary non-tuberculous mycobacterial infections, inspired the hypothesis that parkin knockout mice may provide an improved model.

Methods

A rough morphotype mutant of *M. abscessus* was isolated. Its smooth morphotype parent, was characterized for sensitivity to several promising antimycobacterial drugs, as single agents and in combination, *in vitro* and within infected phagocytes. Mouse strains including C57BL/6J and C3HeB/FeJ, knockouts of *Nos2* and *PARK2*, and a βENaC transgenic were infected with *M. abscessus* by intranasal and intravenous routes. Efficacy of a combination of bedaquiline, clarithromycin, and rifabutin was evaluated in progressive acute infection of C3HeB/FeJ mice.

Results

Whole genome sequencing of the rough morphotype mutant revealed a trinucleotide repeat expansion within the *mps1* gene. The mutant was phagocytosed less efficiently by mouse bone marrow-derived macrophage but showed similar intracellular growth to the smooth morphotype. Combinations of clarithromycin, bedaquiline, and rifabutin demonstrated synergy *in vitro* and decreased viability of *M. abscessus* within infected THP-1 cells, in contrast to growth inhibitory activity of each as a single agent. The rough mutant was cleared from C57BL/6J, *PARK2*$^{-/-}$, *Nos2*$^{-/-}$, and βENaC-Tg mice following intranasal infection, and from *Nos2*$^{-/-}$ and *PARK2*$^{-/-}$following intravenous infection, but at a dose of ~ 3 x 10^6 CFU intravenous C3HeB/FeJ developed a progressive acute infection and survived at least 10 days post-infection. When treated with a combination of bedaquiline, clarithromycin, and rifabutin daily for 7 days, bacterial burden was significantly reduced.

Conclusions

A variety of mouse strains consistently clear *M. abscessus* infections, when established at sub-septic inocula, by both intranasal and intravenous routes. However, at a dose just below one triggering apparent

sepsis, C3HeB/FeJ mice allow establishment of a progressive acute infection, which can be effectively treated with a combination of bedaquiline, clarithromycin, and rifabutin.

Background

Mycobacterium abscessus (*Mab* or *M. abscessus*), originally named *Mycobacterium chelonei* subspecies *abscessus* and recently renamed *Mycobacteroides abscessus*, is a rapidly growing nontuberculous mycobacterium (NTM) that can cause chronic pulmonary infections, particularly in individuals with cystic fibrosis, bronchiectasis, or compromised immune systems [1]. *Mab* is distinguished by its ability to form robust biofilms, persist within lung tissue, and exhibit intrinsic resistance to a wide range of antibiotics. These characteristics make the infection long-lasting, hard to treat, and result in poor patient outcomes despite aggressive treatment regimens [1].

Current therapeutic approaches require combinations of new or repurposed antimicrobial agents, often with limited efficacy and significant side effects [2]. Therefore, the development of more effective drugs and treatment regimens has become a priority, requiring robust preclinical animal models to evaluate experimental antibiotics and enable accurate prediction of clinical trial outcomes.

Mouse models are fundamental to obtain critical insights into pathogenesis and for the evaluation of experimental therapeutic compounds or regimens, due to their relatively small size, low cost, and lesser drug quantities required to conduct *in vivo* efficacy studies. In recent years, a variety of mouse models have been developed to study *Mab* infection. These models differ based on several parameters, including mouse strain/genetic background, the specific *Mab* strain used, route of infection, inoculum dose, use of immunosuppression, target organ, and the duration or persistence of infection [1, 3, 4]. However, despite these efforts, current *in vivo* models present significant limitations in accurately replicating the chronic, progressive pulmonary disease observed in humans [4].

For instance, immunocompetent strains such as C57BL/6 typically clear *Mab* infection rapidly, limiting their effectiveness in modeling long-term or chronic infection. On the other hand, immunocompromised models such as GM-CSF knockout (GM-CSF$^{-/-}$) or SCID mice support chronic infection and granuloma inflammation, however these models are not reflective of the majority of *Mab* patients, who lack overt immunocompromise [1, 3–5]. Chemotherapy is most efficacious in the context of a competent immune response, supporting the predictive value of models that feature both.Various infection routes such as aerosol, intratracheal, intranasal, and intravenous delivery have been used to establish pulmonary infection. Repeated airway challenge or use of modified strains can extend infection duration, yet these models still fail to capture the important features of the disease [1, 3–7].

Given the limitations of models with severe immunocompromise, either genetic or pharmacological, alternatives that may more mechanistically approximate the pulmonary niche of mycobacteria in human patients could prove suitable. One feature that distinguishes mice from humans is the relative contribution of inducible nitric oxide synthase (*Nos2*) to control of mycobacterial infections. In contrast

to the mouse, where IFNγ stimulation results in strong induction of iNOS in macrophages which then control *Mycobacterium tuberculosis* replication through direct antimicrobial action of nitric oxide, human macrophages induce iNOS very weakly or not at all [8]. This difference has recently been leveraged therapeutically; treatment with inhaled nitric oxide was shown to have benefit in the treatment of nontuberculous mycobacterial pulmonary disease (NTM-PD) [9]. Our recent development of a model of tuberculosis that features more human-like lesions using *Nos2*-deficient mice [10] prompted investigation of the potential of that strain for *M. abscessus* infection, despite the previous report of rapid clearance by Obregón-Henao et al. [6].

An additional susceptibility factor for NTM-PD is cystic fibrosis. The difficulty patients with cystic fibrosis have in clearing pulmonary mucus establishes a niche permissive for NTM. The underlying ion transport defects are not reproduced in mice with human cystic fibrosis gene variants, which led to the construction of a transgenic mouse which overexpresses a sodium channel in the pulmonary epithelium [11]. This βENaC-Tg mouse strain develops the pulmonary pathophysiology characteristic of human cystic fibrosis, suggesting it could support a persistent *M. abscessus* infection.

Emerging evidence indicates host genetics contribute to susceptibility to NTM-PD. A recent study identified *PARK2*, encoding the E3 ubiquitin ligase parkin, as a susceptibility gene for NTM-PD infection [7]. The authors demonstrated that individuals with decreased *PARK2* expression are significantly enriched among those with NTM-PD, including those with *M. abscessus* infections, highlighting a critical role of *PARK2* in autophagy regulation and innate immune responses for intracellular pathogen clearance [7].

Prior studies of *M. tuberculosis* infection in *PARK2*$^{-/-}$ (C57BL/6 background) mice have shown that parkin regulates the clearance of intracellular pathogens through mitophagy, and its absence leads to increased bacterial burden and impaired granuloma lesions [12]. *PARK2*$^{-/-}$ knockout mice infected by aerosol exhibited ~ 10-fold higher bacterial loads in lung, spleen, and liver by day 21, and succumbed to infection by day 85 while all wild-type controls survived [12]. Given the convergence of human genetic susceptibility mediated by *PARK2* and the effects of parkin deficiency on tuberculosis infection in mice, we hypothesized that *M. abscessus* infection will be more severe and persistent in *PARK2*-deficient hosts.

We report a test of this hypothesis as well as additional efforts to develop preclinical models of *M. abscessus* infection suitable for evaluation of therapeutic efficacy.

Methods

M. abscessus strains and growth conditions

Mycobacteroides abscessus (Mab) type strain Moore (TMC 1543, derived from ATCC 19977) was obtained from the Trudeau Mycobacterial Culture Collection and cultured in complete 7H9 medium composed of Middlebrook 7H9 broth supplemented with 10% OADC, 0.5% glycerol, and 0.05% tyloxapol

(Thermo Fisher Scientific). OADC was prepared from oleic acid (0.5 g/L; Thermo Fisher Scientific, Waltham, MA), sodium chloride (8 g/L; Fisher Scientific), albumin fraction V (50 g/L; Fisher Scientific, Hampton, NH), dextrose (20 g/L; Fisher Scientific), and catalase (0.04 g/L; Thermo Fisher Scientific). To isolate a rough morphotype mutant (*Mab*-R) from the smooth (*Mab*-S) parental stock, tyloxapol was omitted from the medium to promote aggregation, creating selection pressure favoring growth of the rough morphotype [13, 14]. Cultures were incubated at 37°C with shaking at 150 rpm. After several passages without detergent, cells were plated on 7H10 agar containing 10% OADC and 0.5% glycerol and incubated at 37°C with 5% CO2; colonies with a rough morphology were observed. Strains were grown to mid-log phase, with an optical density at 600 nm (OD_{600}) of 0.4–0.8, then diluted or concentrated to the desired OD depending on the experiment. An OD_{600} of 1.0 was considered equivalent to 3×10^8 colony forming units (CFU) per milliliter.

DNA extraction and whole-genome sequencing (WGS)

Ten milliliter cultures of *Mab* rough and smooth morphotypes were grown to mid-log phase in complete 7H9 medium, and DNA was extracted using the Quick-DNA Fungal/Bacterial DNA MiniPrep Kit (Zymo Research). Libraries were prepared and denatured using the Illumina DNA Prep kit and sequenced on the Illumina MiniSeq system (Illumina). Data analysis was performed using the variation analysis pipeline on BV-BRC [15]

In vitro drug susceptibility assays

Drug susceptibility assays for bedaquiline (BDQ), clarithromycin (CLR), and rifabutin (RFB) were performed as previously described [16] to determine the minimum inhibitory concentration (MIC) of each antibiotic individually. To evaluate drug-drug interactions, 2D and 3D checkerboard assays were carried out in 96-well plates using a checkerboard format and a resazurin-based readout. The fractional inhibitory concentration index (FICI) for each drug pair was calculated as follows: FIC_A = MIC of drug A in combination with drug B / MIC of drug A alone, and FIC_B was calculated similarly for drug B. The FICI was then determined as $FIC_A + FIC_B$. In the 3D checkerboard assay, a fixed concentration of a third antibiotic was added to assess its effect on the 2D drug combination [17]. Drug interactions were interpreted as synergy when FICI $\leq$ 0.5, additivity when FICI >0.5–1, indifferent when 1 < FICI $\leq$ 4.0, and antagonism when FICI > 4.0 [18, 19].

Bone marrow-derived macrophages and THP-1 macrophage-like infection models

Bone marrow-derived macrophages (BMDM) were infected as previously described [12, 20], with slight modifications. BMDMs were isolated from the femurs of C57BL/6J and *PARK2*$^{-/-}$ mice and cultured for 7 days in DMEM (Dulbecco's Modified Eagle Medium) containing 4.5 g/L glucose, L-glutamine, and sodium pyruvate, supplemented with 20% fetal bovine serum (FBS) and 20 ng/mL M-CSF. Cells were then

detached and seeded at a density of approximately 2×10^5 cells per well for 24 h before infection. Cells were infected with *Mab*-S and *Mab*-R at an MOI of 0.1 for 4 h, washed two times with warm 1× PBS (phosphate-buffered saline), and incubated in DMEM supplemented with 10% FBS. At the indicated point, cells were lysed with 0.1% Triton X-100, serially diluted in PBS containing 0.05% tyloxapol (PBS-T), plated on 7H10 agar, and CFU were enumerated after 5 days at 37°C.

Intracellular activity of BDQ, CLR, and RFB was assessed in *Mab*-S-infected THP-1 cells as previously described [16]. Briefly, THP-1 cells were cultured and differentiated into macrophage-like cells with 100 nM PMA for 24 h and infected at a multiplicity of infection (MOI) of 0.1 for 4 h with *Mab*-S. Bacterial viability was measured 3-day post-infection following exposure to the antibiotics alone or in combination. Cells were lysed, serially diluted and plated as described above.

Mouse strains and care

Both female and female C57BL/6J (JAX:000664), *Nos2*$^{-/-}$(JAX:002609), βENaC-Tg (JAX:006438), and *PARK2*$^{-/-}$ (JAX:006582) mice, as well as female C3HeB/FeJ (JAX:00065) mice, aged 6–12 weeks, were used in this study. All strains were originally obtained from The Jackson Laboratory (Bar Harbor, ME) and subsequently bred in-house at Trudeau Institute, except for age-matched C3HeB/FeJ mice, which were purchased directly. All procedures were conducted in accordance with protocols approved by the Institutional Animal Care and Use Committee (IACUC), and animal care, housing conditions, and monitoring were carried out in Trudeau Institute's AAALAC Accredited biosafety level 2 facility. Mice were fed certified, irradiated rodent chow (LabDiet Isopro RMH 3000 5P76) and particulate, UV filtered, acidified (2.5-3.0) water in sterile bottles ad libitum. Mice were housed under SPF conditions in HEPA filtered individually ventilated cages (IVC) and monitored regularly, with body weight measured every other day. Humane endpoints were defined as > 20% weight loss of the pre-experimental weight with signs of distress such as hunched posture, inactivity, isolation, or greasy, severely ruffled fur.

Intranasal (IN) infection

Mice were anesthetized with isoflurane using an induction chamber with active gas scavenging in a certified ventilated Class II B2 biosafety cabinet. The *Mab*-R inoculum was prepared in sterile PBS-T to an OD_{600} of ≥ 1.0, passed through a syringe to disrupt clumps, and 50 µL of the suspension was instilled into the nares. Mice were then returned to their cages and monitored until they were awake and moving normally around the cage.

Intravenous (IV) infection

For intravenous infections, 200 µL of the *Mab* (*Mab*-R or *Mab*-S) suspension, prepared as described previously and adjusted to different OD_{600} values, was injected into the tail vein using a 26-gauge needle.

Drug preparation for in vivo study

For *in vivo* treatment, drugs were administered alone or in combination by oral gavage (200 µL per mouse) at following doses of rifabutin (RFB, 10 mg/kg), bedaquiline (BDQ, 30 mg/kg), and clarithromycin (CLR, 250 mg/kg) daily for a week. RFB and CLR were first dissolved in 100% DMSO and then diluted in 0.5% methylcellulose to obtain a final DMSO concentration of 5%, whereas BDQ was formulated in acidified 20% hydroxypropyl-β-cyclodextrin (HPβCD). All suspensions were sonicated or rotated overnight at 4°C to ensure uniform suspension. Mice treated with 0.5% methylcellulose served as vehicle control and treatment was administered for 1 week.

Viable count of bacterial load in lungs

At the indicated days post-infection, mice were euthanized by CO_2 inhalation, and lungs were aseptically removed and homogenized in 4.5 mL of sterile 0.85% saline using a mechanical homogenizer (Glas-Col Inc., Terre Haute, IN). To determine CFU per organ, lung homogenates were serially diluted in 0.85% saline and plated on Middlebrook 7H11 agar supplemented with OADC, glycerol, with or without 0.4% activated charcoal to prevent BDQ carry-over. Plates were incubated at 37°C, and CFUs were counted after at least 5 days.

Statistical analysis

Statistical analyses were performed using GraphPad Prism version 10 (GraphPad Software Inc., San Diego, CA, USA). Viable CFU counts were $\log_{10}$-transformed prior to analysis and data were analyzed using one or two-way analysis of variance (ANOVA), followed by Dunnett's multiple-comparison test where appropriate. Differences were considered statistically significant at $p < 0.05$.

Results

Isolation of the Mab rough morphotype mutant and WGS analysis

The rough morphotype of *Mab* has been widely associated with increased virulence and persistence, whereas smooth variants are more readily cleared from mouse lungs [6, 21, 22]. To isolate a *Mab* rough morphotype mutant, the parental *Mab* ATCC 19977 smooth morphotype was serially passaged in Middlebrook 7H9 broth supplemented with 10% OADC and 0.5% glycerol, in the absence of tyloxapol. The resulting cultures were then plated on Middlebrook 7H10 agar and incubated at 37°C with 5% CO_2. Colonies displaying the characteristic rough morphology were sub-cultured. Genomic DNA was extracted from cultures of both morphotypes and whole-genome sequencing was carried out to compare the rough mutant with the parental smooth strain to identify genetic variants associated with the morphotype transition. The analysis revealed a single codon expansion of a CTG trinucleotide repeat at nucleotide position 6075 within the *MAB_4099c* (*mps1*) gene. This adds a fourth leucine to a run of three within the encoded non-ribosomal peptide synthase, which has been implicated in glycopeptidolipid (GPL) biosynthesis, required for the smooth morphotype [23].

Intranasal and intravenous mouse infection

Following intranasal infection with *Mab*-R, female and male *PARK2*$^{-/-}$, C57BL/6J, *Nos2*$^{-/-}$, and βENaC-Tg mice were euthanized at 1 and 7 days post-infection to quantify bacterial burden. Across all mouse strains and both sexes, lung bacterial loads decreased by approximately 1 to 2 $\log_{10}$ CFU between days 1 and 7 post-infection (Fig. 1). This uniform reduction in bacterial burden indicated that intranasal inoculation did not establish sustained lung infection in these mice strains under the conditions tested.

CFU were determined on days 1 and 7 post-infection by plating serial dilutions of lung homogenates on 7H11 agar supplemented with glycerol and OADC. Data are presented as mean $\log_{10}$ CFU per lung (n = 5).

To determine whether an alternative route of infection could establish a stable bacterial burden, C3HeB/FeJ, *Nos2*$^{-/-}$and *PARK2*$^{-/-}$ mice were infected intravenously with either the *Mab*-R or *Mab*-S morphotype. We first reproduced the experiment described by Obregón-Henao et al. [6] with minor modification, in which *Nos2*$^{-/-}$ and C3HeB/FeJ mice were intravenously infected with *M. abscessus* strain 103. Female C3HeB/FeJ mice were initially infected intravenously with 200 µL of *Mab*-R at OD_{600} values of 0.01 and 0.1, with an intended study duration of two weeks post-infection. Mice receiving the higher inoculum approached the humane endpoint threshold (≥ 20% body weight loss) by day 7 and were therefore euthanized, with a recorded bacterial burden of ~ 1×10⁶ CFU/lung (Fig. 2A). In contrast, mice infected with the lower inoculum survived to the planned experimental endpoint, with a burden of ~ 4×10^3 CFU/lung (Fig. 2A).

Building on these findings, both male and female *Nos2*$^{-/-}$ mice were subsequently infected intravenously with *Mab*-R at an adjusted OD_{600} of 0.05 and showed an ~ 1–1.5 $\log_{10}$ CFU reduction in lungs bacterial burden between days 2 and 10 post-infection. Notably, a heterogeneous response in bacterial burden across animals was observed at day 10 (Fig. 2B).

Lung bacterial burdens following intravenous infection with *Mab* rough variant in **(A)** C3HeB/FeJ mice (inoculum OD_{600} = 0.01 or 0.1; days 7 and 14 post-infection) and **(B)** *Nos2*$^{-/-}$ mice (inoculum OD_{600} = 0.05; days 2 and 10 post-infection). Data are presented as mean $\log_{10}$ CFU per lung (n = 3–5).

We next evaluated *PARK2*$^{-/-}$ mice infected intravenously with either the *Mab*-R or *Mab*-S morphotype. Three inoculum concentrations (OD_{600} = 0.1, 0.05 and 0.02) were evaluated, and male and female/e mice were combined to obtain a minimum of three to five animals per experimental group. All mice receiving *Mab*-R at inoculum of OD_{600} = 0.1 or 0.05 reached the predefined humane endpoint because of a ≥ 20% loss in body weight and were euthanized before the planned experimental endpoint. The highest initial inoculum (OD_{600} = 0.1) resulted in a lung bacteria burden of ~ 10⁶ CFU on day 3, which declined to ~ 10⁵ CFU/lung by day 6. A similar trend was observed with an initial inoculum of OD_{600} = 0.05, with bacterial burdens decreasing from ~ 5×10⁵ CFU/lung on day 3 to ~ 5×10⁴ CFU/lung by day 6 (Fig. 3).

In contrast, *PARK2*$^{-/-}$ mice infected with *Mab*-R at an OD_{600} of 0.02, as well as all groups infected with *Mab*-S regardless of inoculum, survived until the final experimental time point (Fig. 3). The lung bacterial burden of *Mab*-R at an inoculum OD_{600} of 0.02 declined to approximately 1×10^4 CFU/lung. For *Mab*-S, bacterial burdens decreased in an inoculum-dependent manner, reaching approximately 1×10^4, 5×10^3, and 1×10^3 CFU/lung at OD_{600} values of 0.1, 0.05, and 0.02, respectively (Fig. 3).

Lung bacterial burdens determined on days 3, 6, 9 and 10 post-infection with inocula at OD_{600} = 0.02, 0.05, and 0.1. Data are presented as mean $\log_{10}$ CFU per lung (n = 3–5).

Intracellular infection in BMDM

To assess *Mab* survival in BMDM, we infected control C57BL/6J and Parkin-deficient BMDM with smooth and rough *Mab* morphotypes. At 4 h post-infection, CFU counts differed by two-fold between the two morphotypes, indicating more efficient phagocytosis of the smooth strain (Fig. 4).

Following *Mab*-S infection, no significant difference in intracellular bacteria growth was observed between control and Parkin-deficient BMDM. Relative to the 4-h baseline, CFU increased by 1.9- and 10.5-fold in C57BL/6J BMDM and by 2.3- and 8.3-fold in Parkin-deficient BMDM at 24 and 48 h post-infection, respectively (Fig. 4).

In BMDM infected with *Mab*-R, bacteria replication in C57BL/6J BMDM was comparable to that observed for *Mab*-S, with CFU increasing by 2.6- and 9.7-fold at 24 and 48 h post-infection, respectively. In contrast, Parkin-deficient BMDM restricted *Mab*-R replication, with CFU increasing by 1.5-fold at 24 h and 3.3-fold at 48 h relative to the 4 h baseline (Fig. 4).

Cells were infected for 4 h, harvested at 24 and 48 h post-infection and plated on 7H10 agar. Data are representative of one of three replicate experiments and are presented as mean ± SEM $\log_{10}$ CFU/mL.

Drug-drug interaction analysis and efficacy in a THP-1 macrophage-like ex vivo model and a C3HeB/FeJ M. abscessus progressive acute infection model

Because treatment of *M. abscessus* infection typically requires multidrug regimens rather than monotherapy [24–26], we evaluated the activity of the triple combination of BDQ, RFB and CLA in both *ex vivo* and *in vivo models*. Consistent with prior reports [27], *M. abscessus* exhibited an additive interaction between bedaquiline (BDQ; MIC = 1 μM) and clarithromycin (CLA; MIC = 25 μM), with a fractional inhibitory concentration index (FICI) of 0.625 (Table 1). To determine whether this interaction could be enhanced, rifabutin (RFB), which has been reported to exhibit bactericidal activity against *M. abscessus* [17, 28], was incorporated into a 3D checkerboard assay to determine whether it conferred additional activity beyond the BDQ/CLA combination. In the presence of a sub-MIC concentration of RFB (1/4 × MIC; 0.625 μM), the MIC of the RFB/CLA combination decreased from 6.25 μM to 0.78 μM in the 3D combination. Similarly, the MIC of the BDQ/RFB combination decreased from 0.25 μM to 0.0625 μM in the presence of sub-inhibitory clarithromycin. The calculated FICI for the triple-drug combination was 0.375, indicating a synergistic interaction (Table 1).

Table 1
Drug-drug interaction analysis

Compounds	MIC alone	MIC in combination	FICI	Outcome
CLA	25	3.125	0.625	Additive
BDQ	1	0.5		
CLA/RFB at 0.625 μM	6.25	0.78	0.375	Synergy
BDQ/RFB at 0.625 μM	0.25	0.0625		

FICI values from 3D checkerboard assays of clarithromycin (CLA), bedaquiline (BDQ), and rifabutin (RFB) against *M. abscessus* smooth. MIC was measured on day 3, before the development of inducible clarithromycin resistance.

THP-1 macrophage-like cells infected with *Mab*-S for 4 h and subsequently treated for 72 h with BDQ (2.5 μM), RFB (15 μM), and CLA (125 μM), either as single agents or in combination, exhibited significantly reduced intracellular bacterial burden compared with the DMSO-treated control ($P < 0.0001$; Fig. 5). The RFB/BDQ/CLA triple combination produced a 3.2 $\log_{10}$ reduction in intracellular CFU versus the vehicle control, representing a modestly enhanced effect over the reductions observed with BDQ (1.9 $\log_{10}$), CLA (2.3 $\log_{10}$), or RFB (2.1 $\log_{10}$) alone (Fig. 5).

Bacterial burden was quantified and expressed as $\log_{10}$ CFU/mL and data are presented as mean ± SEM. Statistical significance was assessed using two-way ANOVA followed by Dunnett's multiple-comparisons test, comparing each treatment group with the DMSO control. All treatment groups showed statistically significant differences compared with the DMSO control (∗∗∗∗$P < 0.0001$).

To determine whether the synergistic activity observed *in vitro* translated into enhanced antibacterial efficacy *in vivo*, the BDQ/CLA/RFB combination was evaluated in a C3HeB/FeJ mouse model of *M. abscessus* infection. Briefly, C3HeB/FeJ female mice were infected intravenously with the *M. abscessus* rough morphotype ($OD_{600} = 0.05$) and beginning 2 days post-infection, were treated once daily by oral gavage with rifabutin, bedaquiline, and clarithromycin for 1 week. CFU enumeration showed a ~ 2-fold reduction in bacterial burden in the treated group compared with the vehicle group (Fig. 6).

Data are presented as mean ± SD. Statistical analysis was performed using one-way ANOVA followed by Dunnett's multiple comparisons test (n = 5 per group). Significance is indicated as **** $p < 0.0001$.

Collectively, our findings demonstrate that the combination of rifabutin, bedaquiline, and clarithromycin enhances antimicrobial activity against *M. abscessus* both *in vitro* and in *vivo*.

Discussion

Developing a reproducible immunocompetent mouse model of sustained *M. abscessus* lung infection remains a significant challenge. In this study, we isolated a spontaneous rough mutant of *Mab* ATCC

19977 by serial passage in culture media without tyloxapol. Comparative whole-genome sequencing identified a single detectable genetic difference between the parental smooth and spontaneous rough isolates, consisting of the expansion of a leucine codon repeat in *MAB_4099c*. Also annotated *mps1* or *lgrC_1*, *MAB_4099c* encodes a probable non-ribosomal peptide synthetase located in a genomic region linked to virulence and cell-surface (glycopeptidolipid, GPL) factors in *Mab*; mutations and variation in this locus appear repeatedly in clinical isolates, longitudinal studies and have been reported in association with antibiotic resistance screens (clofazimine) and with persistent/rough morphotype isolates [21, 23, 29–31].

To achieve a higher dose pulmonary infection, we used intranasal inoculation rather than aerosol exposure, which more closely mimics the natural route of infection. Intranasal inoculation of rough morphotype resulted in a rapid decline in pulmonary bacterial burden in all mouse strains tested, including immunocompetent C57BL/6J, *PARK2*$^{-/-}$, *Nos2*$^{-/-}$, and βENaC-Tg mice. An approximately 1 to 2-$\log_{10}$ reduction in lung CFU was observed within the first week after infection depending on host genotype and bacterial morphotype. These findings are consistent with previous reports of gradual bacterial clearance following aerosol infection in immunocompetent mice and highlight the limitations of intranasal inoculation in establishing persistent *M. abscessus* lung infection in immunocompetent hosts [1, 3, 4, 32].

To overcome the limitations of intranasal infection to establish a sustained pulmonary infection with *Mab*, we evaluated intravenous inoculation as an alternative approach. Because our focus was on lung infection, other organs were not collected for bacterial burden assessment, as performed in previous studies [24]. *Nos2*$^{-/-}$ mice infected with *M. abscessus* rough variant recapitulate the bacterial clearance reported by [6], in which complete resolution of infection was observed within 20 days.

Bacterial burdens also declined over time in *PARK2*$^{-/-}$ mice infected with both *Mab* smooth and rough morphotypes, with a dose-dependent reduction in lung CFU observed during the first 10 days post-infection. However, despite a decreasing lung bacterial burden, animals infected with the rough variant reached predefined humane endpoints due to significant weight loss, precluding long-term evaluation of bacterial persistence. Parkin is an important regulator of innate immunity, autophagy, and mitochondrial quality control, and PARK2 deficiency has been implicated in altered host responses to intracellular bacterial pathogens, including *M. tuberculosis* [12]. Despite these reported roles in antimicrobial defense, *PARK2*$^{-/-}$ mice did not exhibit impaired clearance of either the smooth or rough *M. abscessus* variant. Notably, though Parkin-deficient BMDM limited the intracellular replication of *Mab* rough in contrast to *M. tuberculosis* [12], *PARK2*$^{-/-}$ mice were highly susceptible to high-dose infection with the rough variant in the *in vivo* setting.

These findings suggest that PARK2 deficiency alone is insufficient to increase murine susceptibility to *M. abscessus* lung infection under the experimental conditions tested. Because bacterial clearance occurred rapidly, any contribution of Parkin to disease progression may have been masked by the inability of the infection model to establish chronic lung infection.

We took advantage of previously published work demonstrating that C3HeB/FeJ mice intravenously infected with 10^6 CFU of *M. abscessus* 103 exhibit lung bacterial persistence of up to 2.5 $\log_{10}$ CFU for 40 days post-infection [6], and more recently, that bacterial persistence of up to 25 days was achieved following intravenous infection of C3HeB/FeJ mice with the *M. abscessus* rough strain CIP104536T (Pasteur Institute accession of ATCC 19977) [33]. Building on these findings, we infected C3HeB/FeJ mice with our laboratory-isolated *Mab* rough mutant and found that intravenous inoculation at an OD_{600} of 0.1 resulted in sustained bacterial burden to 7 days post-infection; however, substantial weight loss necessitated euthanasia upon reaching predefined humane endpoints. Reducing the inoculum by half allowed bacterial persistence to be maintained to 10 days without morbidity, enabling us to evaluate the synergistic RFB/BDQ/CLA triple combination previously identified *in vitro* via checkerboard assay and intracellularly in THP-1-derived macrophage-like cells. After 7 days, treatment with the triple combination resulted in a statistically significant reduction in bacterial burdens in the lung. Although these findings showed this combination has some promise against *M. abscessus*, further studies should evaluate each antibiotic individually and include standard-of-care agents, such as amikacin, alone or in combination, in this immunocompetent mouse model.

Conclusions

This study highlights the importance of host background, infection route, and inoculum size in establishing *M. abscessus* pulmonary infection in mice.

Rapid bacterial clearance limited the utility of intranasal infection for evaluating persistent infection. Knockouts of *Nos2* and *PARK2*, and a βENaC transgenic showed no benefit in establishing a persistent infection, whereas intravenous infection of C3HeB/FeJ mice with an optimized inoculum maintained pulmonary bacterial burdens. This approach may help establish a robust immunocompetent model for investigating *M. abscessus* pathogenesis and evaluating novel therapeutic interventions.

List of abbreviations

ANOVA Analysis of variance

BDQ Bedaquiline

BMDM Bone marrow-derived macrophages

CF Cystic fibrosis

CFU Colony forming units

CLR Clarithromycin

DMEM Dulbecco's Modified Eagle Medium

FBS Fetal bovine serum

FICI Fractional inhibitory concentration index

GM-CSF Granulocyte-Macrophage Colony-Stimulating Factor

GPL Glycopeptidolipid

HPβCD hydroxypropyl-β-cyclodextrin

IACUC Institutional Animal Care and Use Committee

IVC Individually Ventilated Caging

Mab M. abscessus

Mab-R *M. abscessus* rough

Mab-S *M. abscessus* smooth

M-CSF Macrophage colony-stimulating factor

MIC Minimum inhibitory concentration

MOI Multiplicity of infection

Nos Nitric oxide synthase

NTM Nontuberculous mycobacterium

NTM-PD NTM pulmonary disease

OADC Oleic Acid, Albumin, Dextrose, and Catalase

PBS Phosphate-buffered saline

PBS-T PBS- 0.05% tyloxapol

RFB Rifabutin

SCID Severe Combined Immunodeficiency

SPF Specific Pathogen Free

WGS Whole-Genome Sequencing

Declarations

Ethics approval and consent to participate

Animal studies were approved by the Institutional Animal Care and Use Committee of Trudeau Institute under protocol 18 – 006.

Consent for publication

Not applicable

Competing interests

The authors declare that they have no competing interests.

Funding

This work was partially supported by the National Institutes of Health (grant number R21AI144386). Additional funding was provided by Trudeau Institute. The NIH had no role in the study design, conduct of the research, or preparation of the article.

Author Contribution

G.G.M. isolated the rough morphotype mutant, conducted in vitro and ex vivo drug susceptibility analyses, and mouse infection and treatment studies. T.L-B. assisted with mouse infection and treatment studies. D.D. performed some intravenous infections. B.W. conceptualized the project, performed whole genome sequencing analysis, assisted with mouse infection and treatment studies, supervised, and contributed to funding acquisition. The manuscript was written by G.G.M. and B.W. All authors read and approved the final manuscript.

Acknowledgement

We appreciate the gift of initial breeding stock of PARK2-/- mice from The Jackson Laboratory, facilitated by Dr. Candice Baker, and the efforts of Amanda Schneck and the animal care staff of Trudeau Institute, without whom this work would not have been possible.

Data Availability

All data generated or analyzed during this study are included in this published article or are available from the corresponding author on reasonable request.

References

1. Dartois, V., et al., *Preclinical murine models for the testing of antimicrobials against Mycobacterium abscessus pulmonary infections: Current practices and recommendations*. Tuberculosis (Edinb), 2024. 147: p. 102503.
2. Johansen, M.D., J.-L. Herrmann, and L. Kremer, *Non-tuberculous mycobacteria and the rise of Mycobacterium abscessus*. Nature Reviews Microbiology, 2020. 18(7): p. 392–407.
3. Chan, E.D. and X. Bai, *Animal models of non-tuberculous mycobacterial infections*. Mycobacterial Diseases, 2016. 6(3).
4. Alshiraihi, I.M., et al., *Characterization of new mouse models of acute and chronic Mycobacterium abscessus infection for antimicrobial drug screening*. Antimicrobial Agents and Chemotherapy, 2025: p. e00475-25.
5. Riva, C., et al., *A New Model of Chronic Mycobacterium abscessus Lung Infection in Immunocompetent Mice*. Int J Mol Sci, 2020. 21(18).
6. Obregón-Henao, A., et al., *Susceptibility of Mycobacterium abscessus to antimycobacterial drugs in preclinical models*. Antimicrobial agents and chemotherapy, 2015. 59(11): p. 6904–6912.
7. Park, Y., et al., *PARK2 as a susceptibility factor for nontuberculous mycobacterial pulmonary disease*. Respiratory research, 2024. 25(1): p. 310.
8. Stei, F., et al., *Species-specific iNOS expression distinguishes epithelial and myeloid IFNgamma responses in tuberculosis*. Am J Respir Cell Mol Biol, 2026.
9. Flume, P.A., et al., *Inhaled nitric oxide for adults with pulmonary non-tuberculous mycobacterial infection*. Respiratory Medicine, 2023. 206: p. 107069.
10. Makafe, G.G., et al., *Mouse models of tuberculosis uniformly featuring hypoxic necrotic lesions and poor response to chemotherapy*. Infection and Immunity, 2026. 94(3): p. e00574-25.
11. Zhou, Z., et al., *The ENaC-overexpressing mouse as a model of cystic fibrosis lung disease*. J Cyst Fibros, 2011. 10 Suppl 2: p. S172-82.
12. Manzanillo, P.S., et al., *The ubiquitin ligase parkin mediates resistance to intracellular pathogens*. Nature, 2013. 501(7468): p. 512–516.
13. Howard, S.T., et al., *Spontaneous reversion of Mycobacterium abscessus from a smooth to a rough morphotype is associated with reduced expression of glycopeptidolipid and reacquisition of an invasive phenotype*. Microbiology, 2006. 152(6): p. 1581–1590.
14. Clary, G., et al., *Mycobacterium abscessus smooth and rough morphotypes form antimicrobial-tolerant biofilm phenotypes but are killed by acetic acid*. Antimicrobial agents and chemotherapy, 2018. 62(3): p. 10.1128/aac. 01782–17.
15. Olson, R.D., et al., *Introducing the bacterial and viral bioinformatics resource center (BV-BRC): a resource combining PATRIC, IRD and ViPR*. Nucleic acids research, 2023. 51(D1): p. D678-D689.
16. Makafe, G.G., et al., *A novel chemogenomic discovery platform identifies bioactive hits with rapid bactericidal activity against Mycobacteroides Abscessus*. Tuberculosis (Edinb), 2023. 139: p. 102317.

17. Pryjma, M., J. Burian, and C.J. Thompson, *Rifabutin acts in synergy and is bactericidal with frontline Mycobacterium abscessus antibiotics clarithromycin and tigecycline, suggesting a potent treatment combination*. Antimicrobial agents and chemotherapy, 2018. 62(8): p. 10.1128/aac. 00283 – 18.
18. Huang, Y.-L., et al., *Anti-biofilm activities and antibiotic synergy of naturally occurring compounds against drug-resistant rapidly growing mycobacteria*. Microbiology Spectrum, 2024. 12(8): p. e00199-24.
19. Huang, Y., et al., *Enhanced activity of apramycin and apramycin-based combinations against Mycobacteroides abscessus*. Journal of Antimicrobial Chemotherapy, 2026. 81(1): p. dkaf433.
20. Johnson, B.K., et al., *Macrophage Infection Models for Mycobacterium tuberculosis*. Methods Mol Biol, 2021. 2314: p. 167–182.
21. Catherinot, E., et al., *Hypervirulence of a rough variant of the Mycobacterium abscessus type strain*. Infection and immunity, 2007. 75(2): p. 1055–1058.
22. Byrd, T.F. and C.R. Lyons, *Preliminary characterization of a Mycobacterium abscessus mutant in human and murine models of infection*. Infection and immunity, 1999. 67(9): p. 4700–4707.
23. Pawlik, A., et al., *Identification and characterization of the genetic changes responsible for the characteristic smooth-to-rough morphotype alterations of clinically persistent M ycobacterium abscessus*. Molecular microbiology, 2013. 90(3): p. 612–629.
24. Lerat, I., et al., *In vivo evaluation of antibiotic activity against Mycobacterium abscessus*. The Journal of infectious diseases, 2014. 209(6): p. 905–912.
25. Brown-Elliott, B.A., K.A. Nash, and R.J. Wallace Jr, *Antimicrobial susceptibility testing, drug resistance mechanisms, and therapy of infections with nontuberculous mycobacteria*. Clinical microbiology reviews, 2012. 25(3): p. 545–582.
26. Woods, G.L., et al., *Susceptibility testing of mycobacteria, nocardiae, and other aerobic actinomycetes*. 2011.
27. Ruth, M.M., et al., *A bedaquiline/clofazimine combination regimen might add activity to the treatment of clinically relevant non-tuberculous mycobacteria*. Journal of Antimicrobial Chemotherapy, 2019. 74(4): p. 935–943.
28. Dick, T., et al., *Rifabutin is active against Mycobacterium abscessus in mice*. Antimicrobial agents and chemotherapy, 2020. 64(2): p. 10.1128/aac. 01943–19.
29. Ripoll, F., et al., *Genomics of glycopeptidolipid biosynthesis in Mycobacterium abscessus and M. chelonae*. BMC genomics, 2007. 8(1): p. 114.
30. Rüger, K., et al., *Characterization of rough and smooth morphotypes of Mycobacterium abscessus isolates from clinical specimens*. Journal of clinical microbiology, 2014. 52(1): p. 244–250.
31. Chen, Y., et al., *Novel mutations associated with clofazimine resistance in Mycobacterium abscessus*. Antimicrobial agents and chemotherapy, 2018. 62(7): p. 10.1128/aac. 00544 – 18.
32. Pearce, C.M., et al., *Mycobacterium abscessus pulmonary infection and associated respiratory function in cystic fibrosis-like βENaC mice*. Frontiers in tuberculosis, 2024. 2: p. 1473341.

33. Le Moigne, V., et al., *Efficacy of Bedaquiline, Alone or in Combination with Imipenem, against Mycobacterium abscessus in C3HeB/FeJ Mice*. Antimicrob Agents Chemother, 2020. 64(6).

Figures

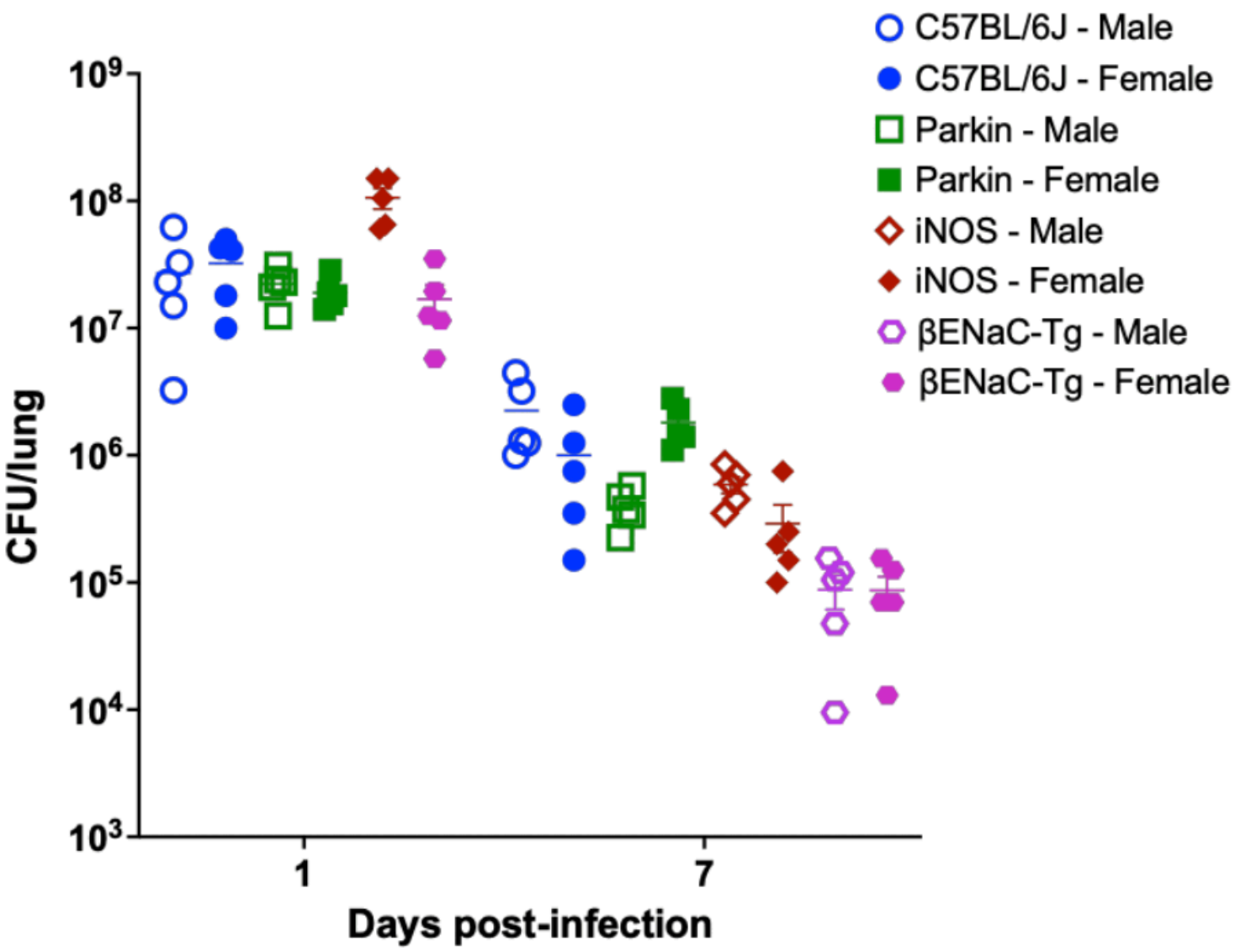

Figure 1

Bacterial burdens in the lungs of C57BL/6J, *PARK2*$^{-/-}$, *Nos2*$^{-/-}$, and βENaC-Tg mice following intranasal infection with *M. abscessus* rough mutant.

CFU were determined on days 1 and 7 post-infection by plating serial dilutions of lung homogenates on 7H11 agar supplemented with glycerol and OADC. Data are presented as mean $\log_{10}$ CFU per lung (n = 5).

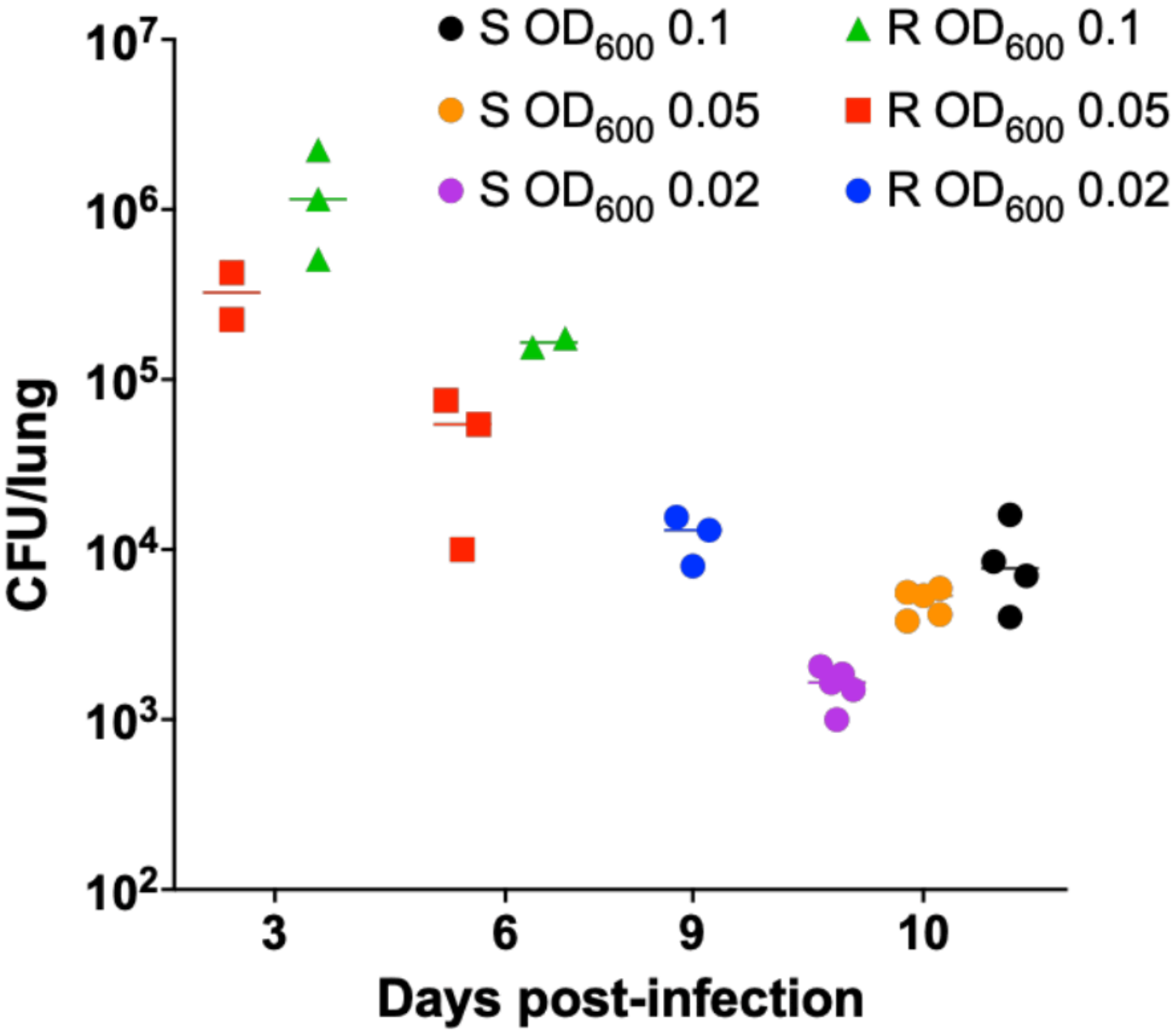

Figure 3

Intravenous infection with *M. abscessus* smooth or rough morphotypes in *PARK2*$^{-/-}$ mice.

Lung bacterial burdens determined on days 3, 6, 9 and 10 post-infection with inocula at OD_{600} = 0.02, 0.05, and 0.1. Data are presented as mean $\log_{10}$ CFU per lung (*n* = 3-5).

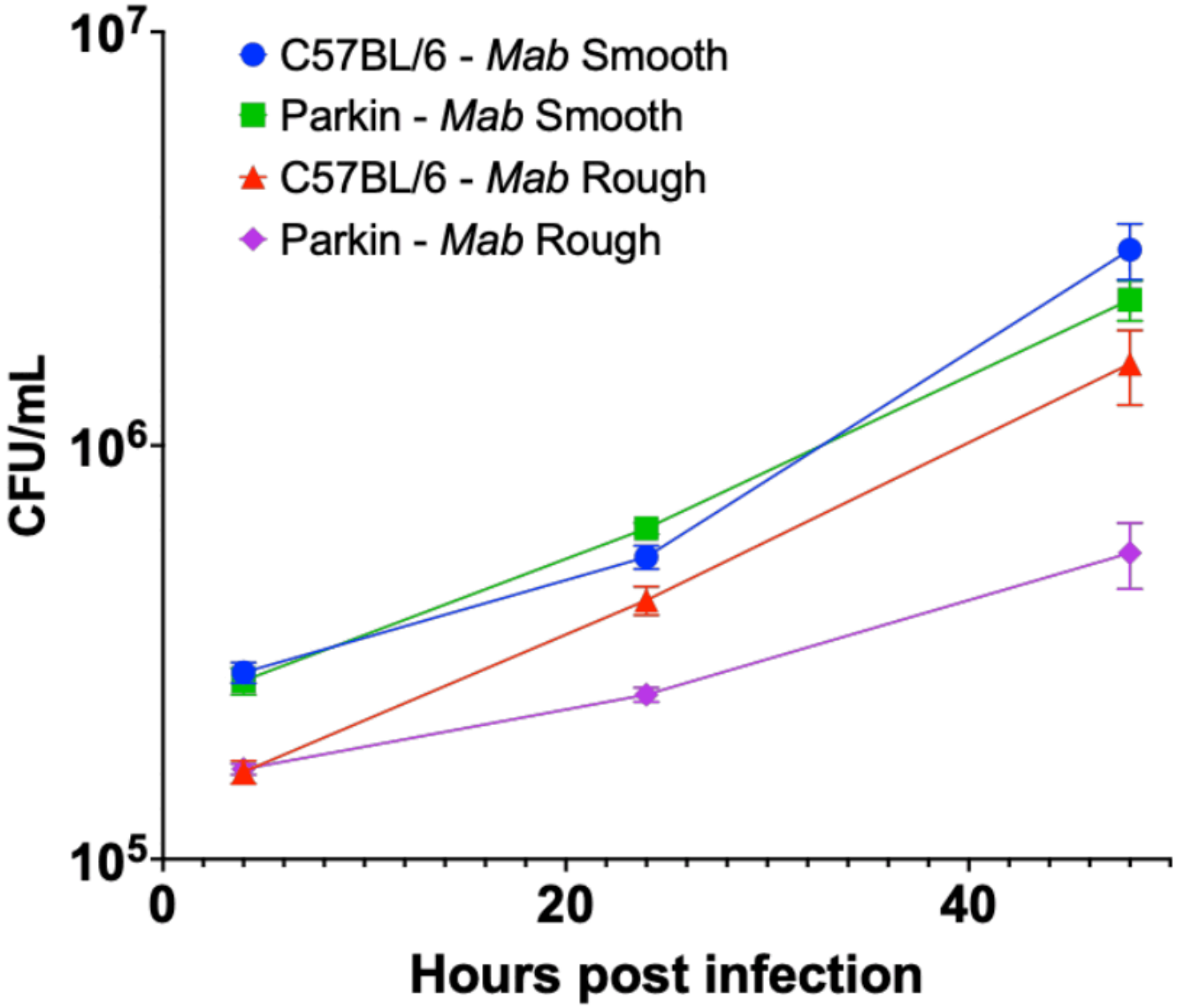

Figure 4

Intracellular growth of *M. abscessus* smooth morphotype in C57BL/6J and *PARK2*$^{-/-}$ BMDM.

Cells were infected for 4 h, harvested at 24 and 48 h post-infection and plated on 7H10 agar. Data are representative of one of three replicate experiments and are presented as mean ± SEM $\log_{10}$ CFU/mL.